ELSEVIER

International Journal of Mass Spectrometry 222 (2003) 243–258

International Journal of Mass Spectrometry

www.elsevier.com/locate/ijms

Performance of a quadrupole ion trap mass spectrometer adapted for ion/ion reaction studies

Gavin E. Reid[1], J. Mitchell Wells, Ethan R. Badman, Scott A. McLuckey*

Department of Chemistry, 1393 Brown Laboratory, Purdue University, West Lafayette, IN 47907-1393, USA

Received 30 April 2002; accepted 3 August 2002

Prepared for the International Journal of Mass Spectrometry in recognition of Jack Beauchamp's distinguished contributions to science and in honor of his 60th birthday.

Abstract

The performance characteristics of a new ion trap system adapted for ion/ion reaction experiments are described. Significantly improved mass analysis figures of merit over previously used ion/ion reaction instrumentation have been realized. For example, the present system has a demonstrated upper mass-to-charge ratio limit of at least 150,000, mass measurement accuracy of better than 200 ppm at $m/z < 20{,}000$, and mass resolving power of better than 1500 at m/z 20,000. The system also has high flexibility with respect to defining MS^n experiments involving both ion/ion reactions and collision-induced dissociation. An experiment is demonstrated involving three distinct ion/ion reaction periods, one collision-induced dissociation step and two ion isolation steps. This experiment has been used to effect the gas-phase concentration, charge state purification, and dissociation of a multiply charged protein ion. Two of the ion/ion reaction periods involved inhibition of the reaction rates of selected ions, referred to as ion parking, whereby resonance excitation is effected during the reaction period. The combination of this high degree of experimental flexibility and improved mass analysis figures of merit over previously used instruments leads to a significantly improved system for the study and application of ion/ion reactions involving multiply-charged ions. (Int J Mass Spectrom 222 (2003) 243–258)

Keywords: Ion/ion reactions; Quadrupole ion trap; Multiply-charged ions; Ion parking; Electrospray ionization

1. Introduction

Gas-phase ion chemistry has played an integral role in both organic and biological mass spectrometry. Unimolecular dissociation has long been used to derive structural information from organic ions and ion/molecule chemistry, *inter alia*, has been used to ionize organic molecules of interest. These chemistries have also been studied for ions derived from bio-molecules, such as proteins, polysaccharides, and oligonucleotides. Indeed, the study of the unimolecular and ion/molecule reactions of biopolymers is a very active area of research. Beauchamp and co-workers have made seminal contributions to current understanding of both unimolecular [1–7] and ion/molecule reactions of bio-ions [8–10]. Among the most powerful tools used to study the chemistries of gaseous bio-ions are ion trapping instruments. Commonly used ion trapping

* Corresponding author. E-mail: mcluckey@purdue.edu

[1] Present address: Joint Protein Structure Laboratory, Ludwig Institute for Cancer Research, Royal Melbourne Hospital, P.O. Box 2008, Parkville 3050, Vic., Australia.

1387-3806/02/$ – see front matter
PII S1387-3806(02)00984-3

instruments include the ion cyclotron resonance (ICR) mass spectrometer, which today is used almost exclusively in conjunction with Fourier transform (FT) techniques for ion detection and manipulation [11–14], and the quadrupole ion trap [15–17]. These instruments are particularly versatile due to the ability to execute experiments involving multiple ion selection steps as well as multiple ion reaction periods ranging in time from one millisecond to many seconds.

While the FTICR and the quadrupole ion trap share many commonalities, there are important differences, both in mass analysis performance and reaction conditions, that distinguish them as tools for the study of gaseous ions. A unique characteristic of the quadrupole ion trap is the facility with which ions of opposite polarity can be stored simultaneously in a common space [18,19]. This characteristic has permitted the study of the reactions of ions of opposite polarity in which at least one of the reactant ions is multiply charged. Such ions are formed readily from biopolymers using electrospray ionization (ESI) [20,21]. Hence, the quadrupole ion trap can be used to study the unimolecular, ion/molecule, and ion/ion reactions of high mass multiply-charged ions [22]. The reactions of multiply-charged ions derived from biopolymers with ions of opposite polarity have been studied both within a quadrupole ion trap [23–31] and within reaction regions external to a mass spectrometer [32–36]. In the latter cases, reactions occur at or near atmospheric pressure in a region in which the two ion polarities are mixed or merged, prior to sampling into the mass analyzer. For example, Loo et al. described studies in which reactions between multiply-charged protein ions generated by ESI and ions of opposite polarity generated by discharge methods or by ESI were effected in a Y-shaped flow tube, where ions generated separately from the two sources were merged and reacted in the base of the Y prior to ion sampling into the vacuum system of the mass spectrometer. The reactants and products were then analyzed with a quadrupole mass filter [32,33]. The relatively limited mass-to-charge ratio range of the mass filter, however, constrained severely the range of ion/ion reaction products that could be analyzed in these studies. More recently, Scalf et al. [34–36] have studied ion/ion reactions between mixtures of multiply-charged protein and oligonucleotide ions formed by ESI and singly-charged ions formed by either polonium decay ionization or corona discharge ionization. The ion/ion reactions proceeded prior to ion sampling into a time-of-flight mass spectrometer with an upper limit in mass-to-charge ratio roughly an order of magnitude greater than that of the mass filter used in the studies of Loo et al. This higher mass-to-charge ratio range has facilitated the study of sequential ion/ion reactions because product ions derived from biopolymers can exceed mass-to-charge ratios of a few thousand. However, with respect to the study of detailed aspects of ion/ion reactions, a major limitation is the lack of mass selection of reactants ions. Also, the ion/ion reaction time is not well controlled or variable, and there is no capability for performing multiple stages of ion/ion reactions throughout an experiment.

The capability of the electrodynamic ion trap for storing simultaneously both positively-charged and negatively-charged ions and its ability to execute multiple step experiments [37,38] make it particularly well-suited for conducting sophisticated experiments involving ion/ion reactions. This capability has been used recently by applying ion/ion proton transfer reactions to the product ions formed from collision-induced dissociation of multiply-charge proteins [29,39–46]. Ion/ion reactions used in this way can simplify interpretation of the product ion spectrum in the course of studying the charge state dependent fragmentation of protein ions. Ion/ion reactions have also been used to form precursor ion charge states for subsequent dissociation that are not produced directly by electrospray [40,42–46]. Furthermore, it has been demonstrated recently that ion/ion reactions of selected protein ion charge states can be inhibited selectively thereby enabling the concentration into a single charge state of much of the charge dispersed initially across multiple protein charge states [47]. This technique, which has been termed “ion parking”, has recently been used to facilitate the gas-phase protein concentration, purification, and dissociation

of selected multiply charged precursor ions from a relatively complex protein mixture [48,49]. Ion trap experiments involving as many as four distinct ion/ion reaction periods as well as a unimolecular dissociation step have been demonstrated [49]. These capabilities have been developed to support new strategies for protein mixture analysis using quadrupole ion trap instrumentation whereby whole protein ions and/or relatively large protein fragments are subjected to tandem mass spectrometry [50,51].

The use of ion/ion reactions in bioanalysis scenarios has involved primarily proton transfer reactions. That is, ion/ion chemistry has been used to manipulate protein parent ion and product ion charge states within the context of a "top-down" approach to mixture analysis. It has been demonstrated that singly-charged anions of fluorocarbons (principally perfluoro-1,3-dimethylcyclohexane, or PDCH) generated by atmospheric-sampling glow discharge ionization (ASGDI) [52] are particularly useful for protein ion charge state manipulation. The anions can be formed by glow discharge in high reproducible yields. Essentially no evidence for either dissociation or adduct ion formation is observed when such anions react with multiply-protonated proteins. The ion/ion chemistry is therefore robust and has made possible the development of the relatively sophisticated MS^n experiments discussed above.

However, within the context of protein analysis, the ion traps used thus far to study ion/ion chemistry have limited analytical performance characteristics. All of the quadrupole ion trap ion/ion reaction experiments reported to date have been performed on home-built quadrupole ion trap systems controlled by Finnigan ITMS electronics and software which were designed largely in the early 1980s. The ITMS system was designed for the analysis of ions of $m/z < 650$ and has been operated far outside its initial performance specifications. Here, we have modified a modern commercially available quadrupole ion trap mass spectrometer equipped with electrospray ionization to allow for ion/ion reactions by injection through the ring electrode of the ion trap of singly-charged ions formed by ASGDI. This system has improved characteristics for analysis of high mass-to-charge ratio ions relative to the original ITMS system and is highly flexible with respect to the number and sequence of ion manipulation and reaction steps that can be programmed. In this report, we describe the measures taken to adapt this ion trap system for ion/ion reactions and summarize its performance characteristics. A series of mass analyzer characteristics [53] including mass-to-charge ratio range, mass resolving power, mass measurement accuracy and MS^n capability are used as the basis for evaluation of the instrumentation.

2. Experimental

Bovine ubiquitin, bovine heart cytochrome *c*, horse heart myoglobin, bovine serum albumin (BSA) and bovine immunoglobulin (IgG) were all purchased from Sigma (St. Louis, MO). The BSA and IgG protein standards were desalted in aqueous 1% acetic acid prior to analysis, using a PD-10 desalting column obtained from Amersham Pharmacia (Piscataway, NJ). All other proteins were used without further purification. Samples were prepared in either aqueous 1% acetic acid or 50:50:1 methanol/water/acetic acid to a final concentration of 2–20 μM prior to introduction to the mass spectrometer.

2.1. Modification of the Hitachi M-8000 ion trap mass spectrometer for ion/ion reactions

All experiments were performed using a Hitachi Instruments Inc. (San Jose, CA) model M-8000 quadrupole ion trap mass spectrometer equipped with electrospray ionization, and modified for ion introduction through the ring electrode by ASGDI, as discussed in detail below. The M-8000 operates at a drive frequency, $\Omega/(2\pi)$, of 770 kHz with a maximum voltage, V_{max}, of roughly 8000 V 0-p. The inscribed radius of the ring electrode, r_0, is 0.707 cm. For sample introduction by conventional electrospray ionization and via nano-electrospray ionization, the standard Hitachi electrospray assembly was removed and the samples sprayed directly into the skimmer

cone of the instrument. Solutions for electrospray were delivered via a syringe pump at a flow rate of 1 μL/min by a length of 100 μm i.d. × 190 μm o.d. fused silica capillary tubing. The electrospray voltage, ranging from +2.0 to +2.5 kV, was applied to the solution via a stainless steel union connected in-line with the fused silica tubing. Nanospray was effected by loading 10 μL of sample solution into a drawn borosilicate glass capillary with a tip diameter of approximately 5–10 μm. The electrical connection to the solution was made by inserting a stainless steel wire through the back of the capillary. Typically, +1.0 to +1.2 kV was applied to the sample needle for nanospray. Fig. 1 shows a diagram (not to scale) of the modified instrument configuration. An ASGDI source was mounted over a 3.75 in. × 2.625 in. hole cut into the top of the vacuum manifold that was centered over the ion trap, with an outer 1/8th in. deep O-ring groove (#244 O-ring). The ASGDI source consisted of a 4.5 in. × 3.5 in. × 1.0 in. stainless steel block with a 2 in. diameter by 0.75 in. deep chamber machined into the top of the source to act as an intermediate pressure region, with a 0.5 in. diameter through hole to the main vacuum chamber of the mass spectrometer. An O-ring-mounted 3 in. diameter × 0.25 in. plate (A1) with a 250 μm aperture hole separated the source region from atmosphere. A 0.25 in. Cajon tube fitting was welded onto A1 to allow introduction of the PDCH reagent vapor (Aldrich). An O-ring-mounted 1.625 in. diameter × 0.1875 in. plate (A2) with a 250 μm aperture hole separated the source region from the main vacuum chamber of the mass spectrometer. The ASGDI source region was evacuated to a pressure of approximately 2 mTorr by a Leybold

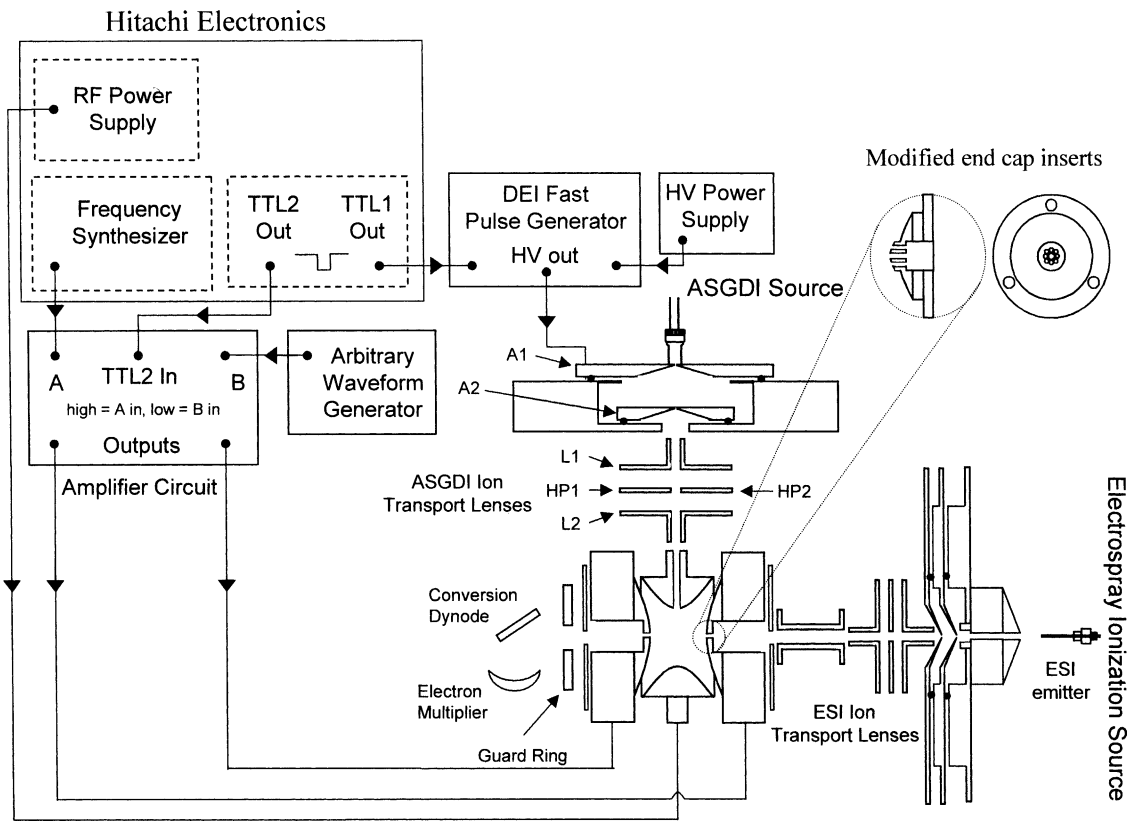

Fig. 1. Schematic diagram of the modified Hitachi ion trap mass spectrometer hardware and electronics circuit configuration. A detailed description of the modifications performed here is given in the Section 2.

D25B rotary vane pump (Leybold Vacuum Products, Export, PA) via two 0.5 in. diameter stainless steel tubes placed in the side of the source. A third 0.5 in. diameter tube was used to connect a convectron gauge (Granville-Phillips, Boulder, CO, model 275) for monitoring the pressure in this region. A series of three DC lenses (L1, HP and L2) with the center lens divided into two "half-plates" (HP1 and HP2) were used to transport and focus ions through the region between the ASGDI source and the ring electrode of the ion trap. A 0.5 in. wide × 0.375 in. deep notch was cut from the outer edge of the ring electrode and a 0.0625 in. hole drilled through the ring to allow introduction of ASGDI derived ions into the ion trap. Potentials of −400, +450, +65, +65 and +60 V were applied to the ASGDI discharge plate (A1) and ion transport lenses L1, HP1, HP2 and L2, respectively, using ORTEC (Oak Ridge, TN) model 556 3 kV (aperture A1) and ORTEC model 710 1 kV quad bias (lenses L1, HP1, HP2 and L2) power supplies.

During operation, the pressure in the ASGDI source region was raised to approximately 800 mTorr by the addition of PDCH vapor in air via a Granville-Phillips variable leak valve (model 203). The main vacuum chamber of the mass spectrometer was evacuated to a pressure of approximately 1×10^{-4} Torr, measured using a Granville-Phillips micro-ion module (model 354) mounted on the vacuum manifold via a 0.5 in. NPT to NW25 flange. Helium was admitted to the region bounded by the ion trap electrodes to a gauge pressure of 1.2×10^{-4} Torr (approximately 1 mTorr corrected pressure) to provide collisional cooling of ions in the ion trap.

For ion/ion reactions, singly-charged negative ions were formed by pulsing the voltage applied to aperture A1 via a DEI (Directed Energy Inc., Fort Collins, CO) model PVX-4150 pulse generator, under the control of a TTL level trigger signal generated by the ion trap (test point T2) and controlled by the ion trap software. Isolation, ion parking [47] and collisional activation of ions of interest was effected via the use of filtered noise fields (FNF's) [54,55] supplied by the Hitachi electronics. A custom-built amplifier circuit with an approximately six times gain was constructed to allow application of user supplied signals to the end-cap electrodes, in addition to those generated by the Hitachi electronics. The amplifier has two analog inputs. The first input was connected to one of the end-cap waveform outputs from the WAVE board of the Hitachi electronics. The amplifier was configured such that the signal from each input yielded two outputs that were 180° out of phase relative to each other, and were directly coupled to the end-cap electrodes. The other end-cap waveform output from the WAVE board of the Hitachi electronics was not used. The second input of the amplifier was connected to an Agilent model 33150 arbitrary waveform generator (Agilent Technologies, Palo Alto, CA) to supply a DC offset, under the control of a TTL level signal (test point T16) via the ion trap software, to the end-cap electrodes at selected times during the experiment to improve high mass ion ejection efficiencies. The amplifier was configured to supply positive DC to one of the outputs and negative DC to the other.

Mass analysis was performed via resonance ejection, at a frequency selected to give the desired mass range extension [56,57]. The application of resonance ejection frequencies for mass analysis at extended mass ranges was achieved using custom software supplied by Hitachi. To enable efficient resonance ejection of high mass ions, the end-cap electrodes were modified by replacing the standard end-cap aperture inserts with custom inserts, which were shaped to correspond to the measured end-cap hyperbole. The curved inserts had a central hole of 0.04 in. diameter surrounded by eight additional evenly spaced holes of 0.0225 in. diameter on a 0.0825 in. bolt circle. In addition, a 1.5 in. diameter × 0.75 in. guard ring electrode with a 0.25 in. through hole was placed between the exit end-cap electrode and the conversion dynode to enhance further the sensitivity for high mass ions. A Tennelec (Canberra Industries, Meriden, CT) model TC950A 5 kV high voltage power supply was used to supply −1.0 kV to the guard-ring. All data shown were collected under conditions selected to obtain spectra with optimal signal-to-noise ratio, and were the average of 100–1000 scans.

Data for ubiquitin were acquired also with an older ion trap system to compare and to contrast with data collected with the Hitachi system. The older system is an electrospray ion trap modified for ion/ion reactions based upon Finnigan (San Jose, CA) ITMS electronics and ICMS software [58]. The instrument has been described in detail [59] and the conditions used to acquire the post-ion/ion reaction MS/MS data for ubiquitin ions have been described elsewhere [42].

3. Results and discussion

3.1. Mass analysis figures of merit

The Hitachi M-8000 instrument is an electrospray ion trap mass spectrometer designed to support an upper mass-to-charge ratio limit of 2000. Several approaches have been used to reach upper limits to m/z ratio well in excess of 2000 using quadrupole ion traps. These include, the reduction of the ion trap radius [57], increasing the amplitude of the radio frequency (RF) drive voltage [60], operation at relatively low trapping RF [61,62], and resonance ejection [56,57]. Reducing the ion trap radius results in a decrease in ion storage capacity, which is undesirable in most applications. There are practical constraints related to electrical breakdown associated with increasing the amplitude of the RF drive voltage. Therefore, the most attractive means for extending significantly the mass-to-charge ratio range of the ion trap are to reduce the frequency of the RF drive voltage, to employ resonance excitation to eject ions at low q_z values, or both. The highest mass-to-charge ratios reported to date for which ions have been analyzed with a quadrupole ion trap have been demonstrated with ion traps operated at low radio frequencies. For example, Schlunegger et al. demonstrated the analysis of singly-charged ions of mass-to-charge approximately 150,000 with a MALDI/ion trap operated at frequencies less than about 100 kHz whereby the mass spectrum was acquired by scanning the RF while maintaining a fixed amplitude [61]. Cai et al. have demonstrated the analysis of microspheres of mass-to-charge ratio in the range of 10^6–10^{10} using an audio-frequency ion trap (<1 kHz) and a laser scattering detection technique [62]. However, the use of low trapping frequencies can compromise mass resolution as well as other aspects of an ion trap MS^n experiment by reducing the secular frequency range of the stored ions.

Of the possible approaches that might be considered for extending the mass-to-charge ratio range of the M-8000, resonance ejection is by far the simplest. The only requirement is to be able to apply the appropriate frequency to the end-cap electrodes. Furthermore, resonance ejection does not compromise any other aspects of an MS^n experiment. All ion/ion studies reported to date have been executed using ion traps of trapping frequency = 1.1 MHz, ring electrode radius (r_0) = 1.0 cm, and $V_{0\text{-p}}$ = 0–7500 V. Singly-protonated BSA (m/z 66,000), for example, has been observed following an ion/ion reaction period via resonance ejection in such an ion trap [27], but at very low relative abundance. A significant decrease in ion storage efficiency that has been noted beyond a mass-to-charge ratio value of roughly 30,000 has been attributed, at least in part, to an increasingly weak trapping field as the mass-to-charge ratio of an ion increases under a fixed set of ion storage conditions. A related issue is the size of the stored ion cloud, which is largely determined by the strength of the trapping field, relative to the area of the ion exit aperture(s). The "effective" potential trapping well for an ion can be estimated using the pseudopotential well approximation [63] which, for the axial dimension, considers the ion to execute its motion in a potential well-depth of

$$D_z = -\frac{eV^2}{4mr_0^2\Omega^2} \quad (1)$$

where D_z is the axial-dimension well-depth for a singly-charged ion, V the amplitude of the RF applied to the ring electrode (0-p), m the mass of the ion, r_0 the inscribed ring electrode radius, and Ω is the angular frequency of the RF voltage applied to the ring electrode. In the radial-dimension, the trapping potential well-depth is half that in the axial dimension. This approximation is most valid for ratios of $eV/(mr_0^2\Omega^2)$

less than about 0.4. The high mass-to-charge ratio ions relevant to this work are well within the range for this approximation to be valid.

The M-8000, with its smaller radius and lower Ω, is expected to provide deeper pseudopotential trapping wells for a given value of V and should therefore provide improved high mass-to-charge ratio performance relative to the previously used ITMS-based ion traps. This has proved to be the case, as illustrated in Fig. 2. Fig. 2A shows the post-ion/ion reaction mass spectrum of BSA acquired with a resonance ejection frequency of 6 kHz, which yields a nominal upper mass-to-charge ratio limit of 81,000. (The frequencies of 1–9 kHz were made accessible to us by Hitachi as the instrument was delivered originally with a lower frequency limit for resonance excitation of 10 kHz). The inset shows an expansion of the mass-to-charge ratio region encompassing the singly-charged ion. The peak width at half height, 390 Da, suggests that the resolving power obtained under these scan conditions is 150–200 based on the isotopic distribution of the 66.4 kDa protein. (Note that the sharp peaks that define the signal envelope arise from the fact that the ions are being ejected at a lower frequency than the signal is being digitized. The width of the sharp peaks is not a reflection of the mass resolving power.) A precise determination of resolving power is complicated by the possibility for protein heterogeneity and the presence of metal ions, which would make the inherent peak width more broad. In any case, the peak width observed here is only 25–50% of that observed on the older instrumentation [59] and the absolute and relative abundance of the singly-charged ion is at least an order of magnitude greater than ever observed in previous post-ion/ion reaction experiments.

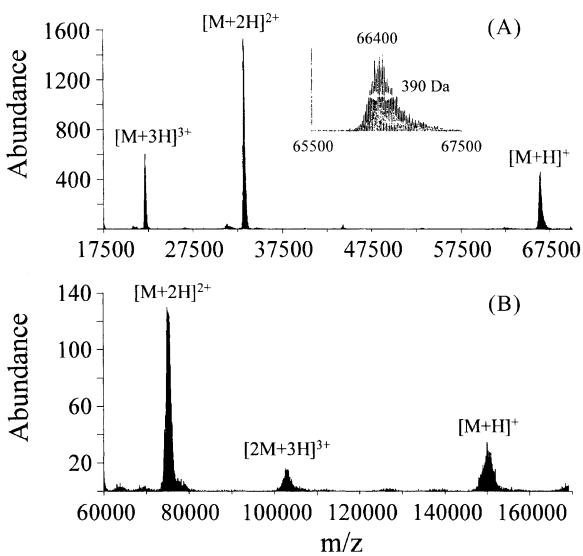

Fig. 2. Post-ion/ion reaction mass spectra of (A) bovine serum albumin, and (B) bovine immunoglobulin IgG, acquired at 6 kHz, and 3 kHz resonance ejection frequencies, to give an upper mass-to-charge ratio limit of approximately 81,000 and 169,000, respectively. The inset to part 'A' contains an expanded mass-to-charge ratio region surrounding the $[M + H]^+$ ion and includes the measured peak width at half height and calculated mass resolution.

The data of Fig. 2A suggest that the effective upper mass-to-charge ratio limit of the system is significantly greater than 67,000. The largest species for which post-ion/ion reaction data have been collected is bovine immunoglobulin, IgG, a 150 kDa protein (Fig. 2B). The data were collected using a resonance ejection frequency of 3 kHz, which yields an approximate upper mass-to-charge ratio limit of 169,000. Note that dimer formation is evident from the ion signals corresponding to the $[2M + 3H]^{3+}$ ion. Therefore, the signals labeled as $[M + 2H]^{2+}$ and $[M + H]^+$ also likely reflect contributions from $[2M + 4H]^{4+}$ and $[2M + 2H]^{2+}$, respectively. Note that no signals corresponding to $[2M + H]^+$ were observed at lower resonance ejection frequencies. Furthermore, the abundance of the nominally singly-charged ion population could not be made to increase significantly with longer ion/ion reaction times. This behavior is consistent with poorer ion storage and/or ejection efficiency for the singly-charged ion relative to the doubly-charged ion. Similar behavior for BSA ions has been observed with the older ion trap instrumentation. Therefore, the Hitachi system appears to show a significant decrease in performance (ion storage and/or ejection efficiency) above roughly m/z 75,000 whereas the older system showed a significant decrease in performance above roughly m/z 30,000.

The M-8000 operates with a fixed scan rate for the RF voltage amplitude. However, the effective mass

scan rate is a function of the resonance ejection frequency such that an extension of the upper limit of the mass-to-charge ratio range by a factor of two results in a similar increase in the mass scan rate. Furthermore, the ion signals are digitized at a constant rate such that the number of data points per peak decreases with increasing mass range extension factor. The increase in mass scan rate and decrease in the number of data points per mass are expected to result in a decrease in mass resolving power as the mass-to-charge ratio range is extended. This is illustrated with the post-ion/ion reaction mass spectra of bovine ubiquitin (Fig. 3A), bovine cytochrome *c* (Fig. 3B), and horse heart apomyoglobin (Fig. 3C). The mass spectra were acquired at resonance ejection frequencies of 53 kHz (upper $m/z \cong 9000$), 37 kHz (upper $m/z \cong 12{,}800$), and 27 kHz (upper $m/z \cong 17{,}600$), respectively. Approximate values for the resolving powers associated with the various mass analysis conditions, as determined by full width at half maximum for the $[M+H]^+$ ions are 2379, 1912 and 1615, respectively. These values are factors of 3–5 times higher than those observed in spectra acquired with the older instrumentation (data not shown). Furthermore, mass measurement accuracies in the range *m/z* 5000–20,000 have been observed to be consistently less than 200 ppm using external mass calibration. Mass measurement accuracies of roughly 300 ppm are typical with the older instrumentation for the same mass-to-charge ratio range. This improvement in mass accuracy is due, at least in part, to the fact that the Hitachi detection system digitizes ion signals at a rate eight times higher than that of the older system. This higher digitization rate leads to an improved ability to determine peak location when the mass-to-charge range is extended significantly by resonance ejection. Hence, the mass analysis performance of the M-8000 is superior to that of previous instrumentation in terms of the key mass analysis figures of merit, i.e., mass resolving power, mass measurement accuracy, and mass-to-charge ratio range.

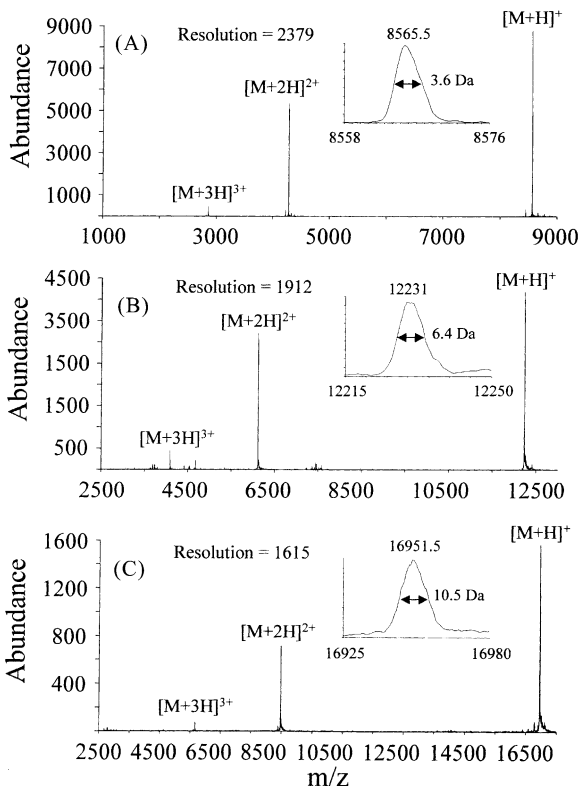

Fig. 3. Post-ion/ion reaction mass spectra of (A) ubiquitin, (B) cytochrome *c*, and (C) myoglobin, acquired at 53, 37 and 27 kHz resonance ejection frequencies, to give upper mass-to-charge ratio limits of approximately 9000, 12,800 and 17,600, respectively. The insets to each figure contain an expanded mass-to-charge ratio region surrounding the $[M+H]^+$ ion and include the measured peak width at half height and calculated mass resolution in each case.

3.2. MS^n performance

A high degree of flexibility in defining MS^n experiments is necessary to maximize the range of possible ion chemistry studies that combine different types of reactions (e.g., unimolecular dissociation and ion/ion reactions). The M-8000 allows for a high degree of flexibility in defining the various steps that go into an ion trap MS^n experiment. For example, readily controlled variables include the amplitude of the RF, the time of a step (essentially from 1 ms to 10 s), and the application of operator-defined FNFs. Furthermore, various events can be triggered during a step, such as negative ion accumulation, application of supplementary DC to the end caps etc. Ion isolation and ion activation are effected via FNFs. The system provides

frequencies from 1 to 500 kHz at 1 kHz spacings. Selective removal of frequencies from the full frequency spectrum allows for ion isolation while the application of selected frequencies from the available frequency spectrum can be used to excite selectively or to eject ions of particular mass-to-charge ratios. We found that the FNFs supplied currently by the electronics are not fully effective at ejecting ions higher in mass-to-charge ratio than the ion being isolated. Removal of the residual high mass-to-charge ratio chemical noise was effected, therefore, by the application of a small DC field across the end-cap electrodes (see Section 2). Pseudopotential trapping well-depth is inversely related to mass-to-charge ratio (see Eq. (1)). An increasing DC potential across the end-cap electrodes therefore can serve to remove ions from the ion trap in the order of high mass-to-charge ratio to low mass-to-charge ratio. In this section we illustrate the performance of the system for several key types of MS/MS and MS^n experiments.

The use of ion/ion proton transfer reactions for manipulating precursor and product ion charge states facilitates greatly the study of whole protein ions in the quadrupole ion trap [22–30,39–53]. For example, a key experiment in studying the charge state dependent fragmentation behavior of whole protein ions in the quadrupole ion trap is to apply ion/ion proton transfer reactions to product ions formed via ion trap collisional activation [29]. By converting all product ions largely to the +1 charge state, any possible charge state ambiguities associated with the product ions initially formed are resolved and the relative contributions of the various dissociation channels can be evaluated without having to consider charge state dependent ion detection efficiency. A typical experiment involves isolation of a parent ion charge state of interest, collisional activation to form product ions, ion/ion proton transfer reactions to yield largely singly-charged products, and mass analysis of the products. Results from such an experiment involving the $[M + 7H]^{7+}$ ion of ubiquitin acquired with the older Finnigan ITMS-based system and with the modified Hitachi instrument are compared in Fig. 4A and B, respectively. Two important observations can be drawn from this comparison. First, the superior resolving power of the newer instrument, by a factor of 3–4, is obvious, as is most clearly seen in the *m*/*z* 6400–7400 regions (Fig. 4C and D) derived from the spectra of Fig. 4A and B, respectively. For example, relatively small signals arising from ammonia losses from the various product ions are resolved in Fig. 4B whereas the contributions from the same losses appear as either shoulders or are buried under the low mass-to-charge ratio side of the respective y-type fragments in Fig. 4C. Second, the mass-to-charge ratios and relative abundances of the product ions in the two spectra are remarkably alike. Similar observations have been made for other protein ion charge states in cases in which direct comparisons could be made. Therefore, the general trends observed regarding the dissociation of multiply charged protein ions in the older ion trap instrumentation are expected to be valid in the newer instrument. Extensive effort to adjust ion activation conditions to obtain such similar looking spectra was not necessary. The reproducibility of product ion spectra obtained on the older instrumentation over a period of several years has been excellent. The comparison shown here suggests that the reproducibility of protein product ion spectra obtained via ion trap collisional activation can be very good even between different ion trap systems.

Another important experimental tool for an ion trapping system capable of effecting ion/ion reactions is the ability to inhibit selectively the rate of ion/ion reactions. This capability has been illustrated recently with the older system [47] and is referred to as ion parking. It can be accomplished, for example, via the resonance excitation of a particular ion during the period in which ions of opposite polarities are stored simultaneously. The ion/ion reaction rate for the accelerated ion is reduced greatly due to both a decrease in the spatial overlap of the oppositely-charged ion reactants and an increase in the relative velocity of the ion–ion pair. An important application of ion parking is the accumulation of ions of several, or even all, charge states formed initially by electrospray into a single charge state. This is, in effect, a gas-phase protein ion concentration process. The ion parking

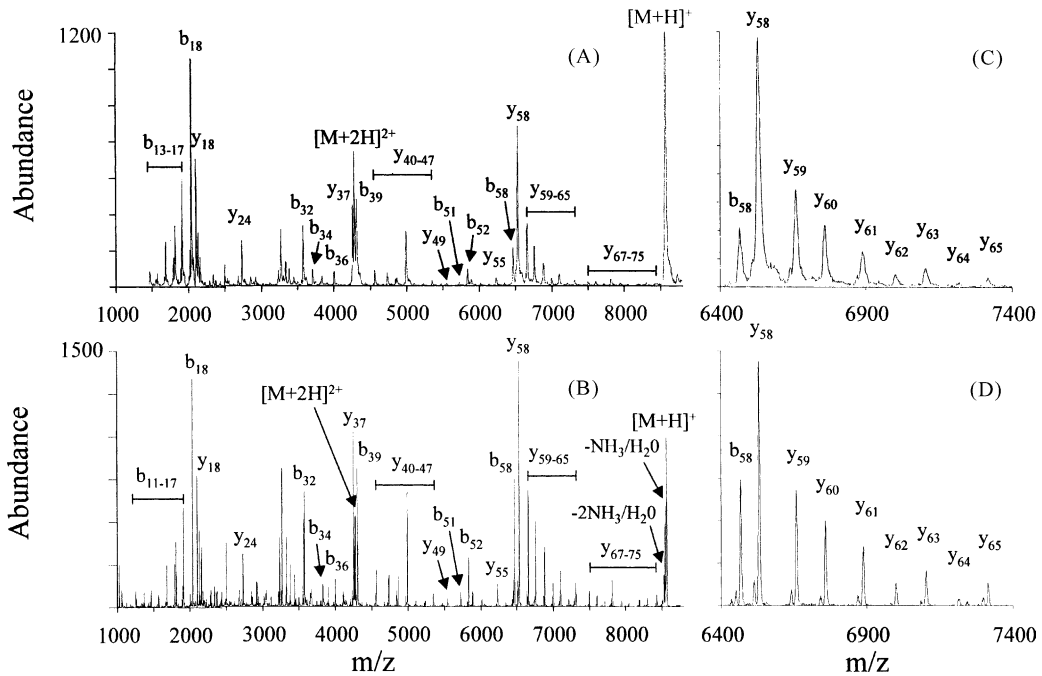

Fig. 4. Post-ion/ion reaction CID MS/MS spectra of the $[M + 7H]^{7+}$ ion of ubiquitin obtained on (A) Finnigan ITMS and (B) Hitachi model M-8000 mass spectrometers. The spectra shown in (C) and (D), show expanded mass-to-charge ratio regions from 6400 to 7400 of the data in A and B, respectively.

experiment is illustrated here with BSA. The mass spectrum obtained following introduction of the BSA sample at a concentration of 10 μM in a solution of 50:50:1 methanol/water/acetic acid by nanospray ionization is shown in Fig. 5A. Approximately 20 charge states of BSA, ranging from $[M + 35H]^{35+}$ to $[M + 59H]^{59+}$ were observed. Following ion/ion reactions for a short period of time (300 ms) in the absence of ion parking, the initial charge state distribution was reduced to approximately 10 charge states ranging from $[M + 17H]^{17+}$ to $[M + 27H]^{27+}$ (see Fig. 5B). Note however, that only an approximately two-fold increase in ion abundance was observed for any of the individual charge states. As shown in Fig. 5C, upon application of a resonance excitation frequency of 18 kHz during the ion/ion reaction period, effective accumulation of the entire ion population into a single charge state ($[M + 34H]^{34+}$) of BSA was observed, resulting in an approximately 20-fold increase in the ion abundance. By normalizing the abundance scales between the three spectra, it is estimated that almost quantitative concentration of the initial ion population into the +34 charge state was achieved.

The ability to "park" essentially all of the BSA signal, which was initially dispersed over roughly 20 charge states, into a single charge state has obvious practical utility for subsequent MS^n experiments. It is important to recognize, however, that the ion parking procedure leads to the inhibition of ion/ion reactions for all ions within the mass-to-charge ratio window subjected to resonance excitation. This can be particularly problematic when a mixture of proteins is present initially because charge states of different proteins can be accumulated within the same parked ion population. Subsequent activation of such an ion population would lead to a product ion spectrum with contributions from multiple proteins of different mass and charge but similar mass-to-charge ratio.

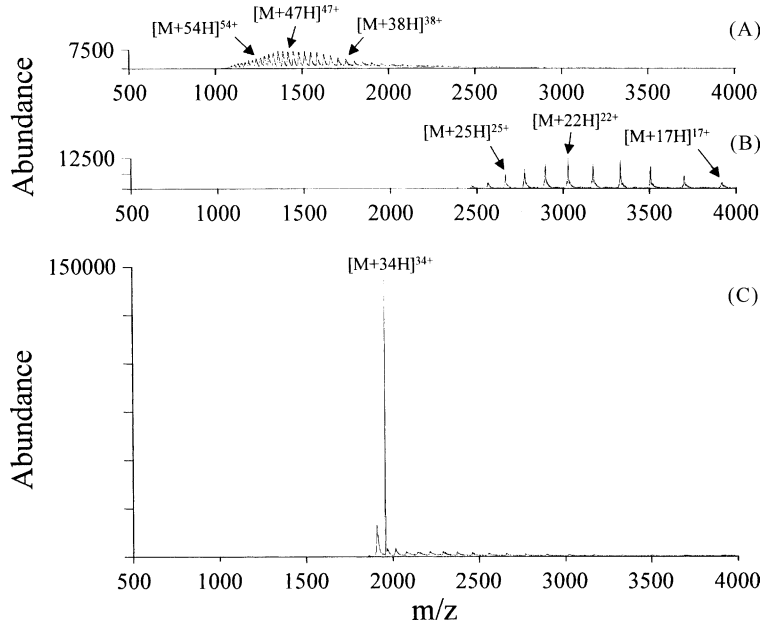

Fig. 5. Ion parking of bovine serum albumin (BSA). (A) Mass spectrum of BSA obtained following introduction of the sample to the mass spectrometer by nanospray ionization. (B) Mass spectrum obtained following a short ion/ion reaction period of the ions in 'A'. (C) Mass spectrum obtained upon application of a resonance excitation frequency of 18 kHz during an identical ion/ion reaction period as shown in 'B' to effect ion parking of the $[M + 34H]^{34+}$ charge state of BSA.

Therefore, it is desirable to be able to "charge state purify" a parked ion population such that only proteins within a particular "mass window," as opposed to a "mass-to-charge ratio window," are subjected to ion activation. This can be done by sequential ion parking via the use of two ion parking periods in conjunction with two ion isolation steps. The first ion parking period is used to accumulate ions into a selected mass-to-charge ratio window, and an ion isolation step is then used to eject ions outside of this window. A second ion parking period is then used to accumulate ions present in the isolated population into a second mass-to-charge ratio window which encompasses, for example, the mass-to-charge ratio of the next lower charge state of the protein of interest. Proteins of different mass and charge in the original parked ion population will move to mass-to-charge ratios other than that of the second parked ion population and can then be removed by a second ion isolation step.

This multiple ion parking/ion isolation process serves to concentrate and to charge-state purify an ion population for subsequent interrogation by collisional activation. The process is illustrated in Figs. 6 and 7, which also demonstrate the efficiency of the sequential ion parking procedure, defined as the fraction of the initial reactant ion population that can be accumulated into a specific charge state following the two ion/ion reaction and ion isolation steps. (A precise measure of efficiency is complicated by a lack of quantitative information regarding detector response dependence on protein charge state. However, the charge state normalized total ion signals represented by Fig. 6A–D are comparable suggesting that, at least over the charge state range reflected in Fig. 6, an assumption of linear detection efficiency with respect to charge state is reasonable.) Fig. 6A shows the pre-ion/ion electrospray mass spectrum of cytochrome *c* obtained after introduction of the sample by nanospray ionization. Fig. 6B shows the

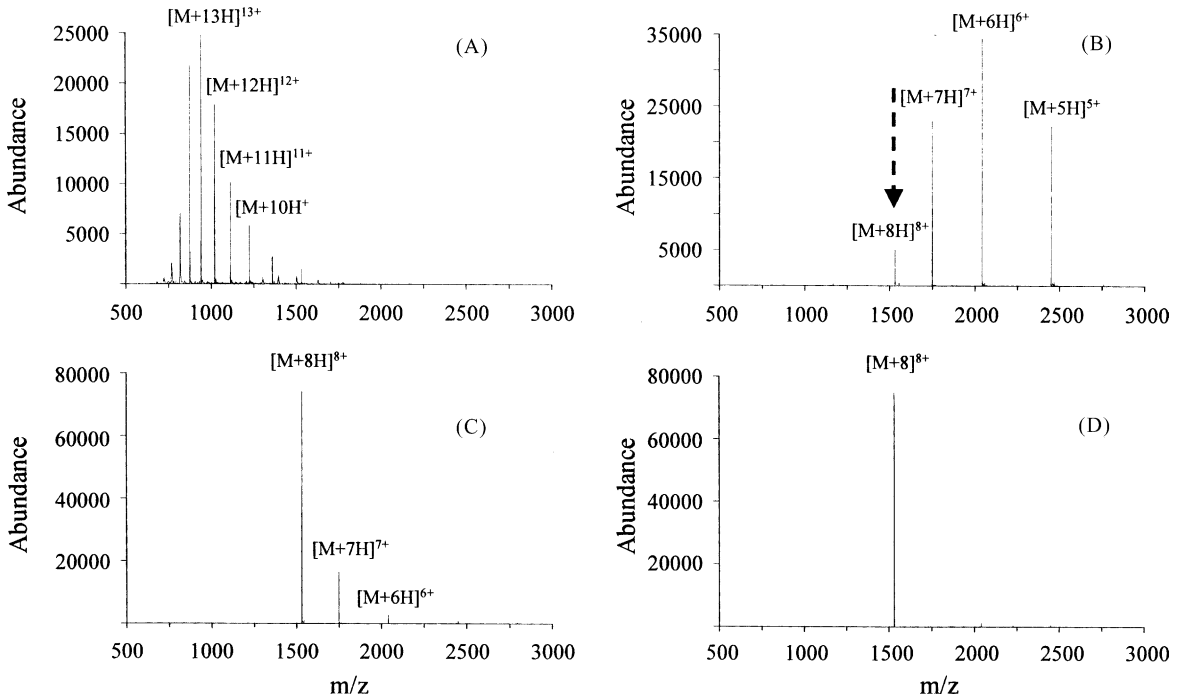

Fig. 6. Concentration of selected multiply protonated protein ion charge states by ion parking. (A) The mass spectrum of cytochrome *c* obtained following introduction to the mass spectrometer. (B) Product ion spectrum obtained after a short anion accumulation and mutual ion storage reaction period of the ions shown in 'A'. (C) Ion parking of the $[M + 8H]^{8+}$ ion of cytochrome *c*, using the same ion/ion reaction conditions as those used in 'B'. (D) Isolation of the concentrated $[M + 8H]^{8+}$ ion.

post-ion/ion mass spectrum (no ion parking) after a short anion accumulation and mutual ion storage reaction period. Fig. 6C shows the spectrum obtained upon application of single frequency resonance excitation during the ion/ion reaction period to effect ion parking, using the same ion/ion reaction conditions as those used in Fig. 6B. The parked $[M+8H]^{8+}$ ion was then isolated (Fig. 6D). It is apparent from Fig. 6C that few, if any, ions are lost as a result of the ion parking process as the total ion abundances in Fig. 6A–C are comparable. However, the ion parking process was not 100% effective because some charge states lower than the parked ion were observed. After the final ion isolation step, it is estimated that only 10–15% of the initial protein ion population, represented by the $[M + 7H]^{7+}$ and $[M + 6H]^{6+}$ ions, is lost.

In order to purify cytochrome *c* ions from low level contaminants, the concentrated $[M + 8H]^{8+}$ ions were subjected to further ion/ion reactions to reduce its charge state. Fig. 7A shows the product ion spectrum obtained after a short anion accumulation and ion/ion reaction period on the isolated $[M + 8H]^{8+}$ ion. Fig. 6B shows the spectrum obtained upon application of single frequency resonance excitation during the ion/ion reaction period to effect ion parking of the $[M + 7H]^{7+}$ ion, using the same ion/ion reaction conditions as those used in Fig. 7A. The parked $[M + 7H]^{7+}$ ion was then isolated (Fig. 7C), and then reduced primarily to its +1 charge state by a final ion/ion reaction period (Fig. 7D). Because approximately equal ion abundances were observed for both the +8 and +7 ion populations following their respective ion parking reactions, almost no ions were lost in reducing the cytochrome *c* ion population from the +8 charge state to the +7 charge state. The overall process illustrated in Figs. 6 and 7 show, therefore,

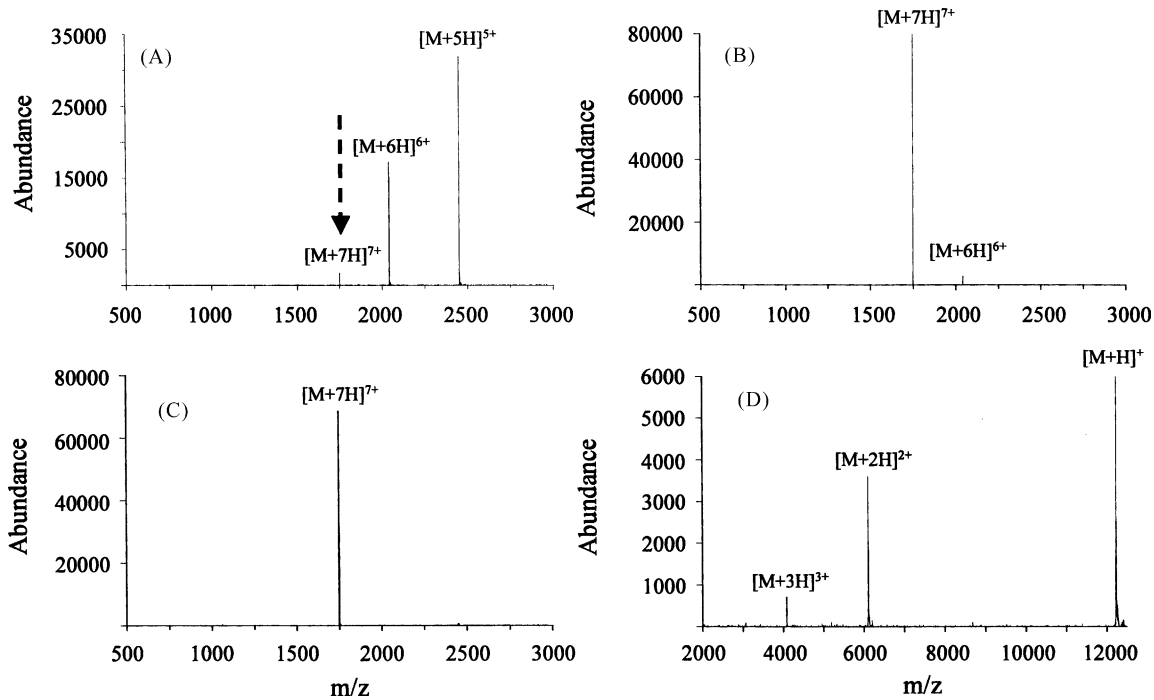

Fig. 7. Purification of selected multiply protonated protein ion charge states by sequential ion parking. (A) Product ion spectrum obtained after a short anion accumulation and ion/ion reaction period of the concentrated $[M + 8H]^{8+}$ ion shown in Fig. 6D. (B) Ion parking of the $[M + 7H]^{7+}$ ion of cytochrome *c*, using the same ion/ion reaction conditions as those used in 'A'. (C) Isolation of the concentrated $[M + 7H]^{7+}$ ion. (D) Product ion spectrum of the concentrated and purified $[M + 7H]^{7+}$ ion of cytochrome *c*, following ion/ion reactions to reduce the charge states primarily to the singly-charged state. The spectrum in 'D' was acquired under the same conditions as described in Fig. 3B.

that an ion population present initially over a range of charge states can be concentrated into a single "purified" charge state with little absolute ion loss.

The capabilities illustrated in Figs. 4–7 are all used within a single process when a protein ion is subjected to ion activation after the concentration/purification procedure, and the product ions are then converted subsequently to singly-charged ions by ion/ion reactions prior to their mass analysis. Fig. 8 shows the product ion spectrum obtained after the concentrated and purified $[M + 7H]^{7+}$ ion of cytochrome *c*, as represented in Fig. 7C, is subjected to ion trap collisional activation and the products are subjected to ion/ion proton transfer reactions. The product ions and abundances are the same as observed previously for the dissociation of multiply charged cytochrome *c* ions [45], but the resolution is again significantly better than observed previously. For example, the loss of multiple small molecule losses from the precursor ion, as well as from many of the product ions, can be readily determined. The main point of this spectrum, however, is that its collection involved two ion parking periods, two ion isolation periods, an ion activation step, and an ion/ion reaction period to manipulate product ion charge states. A total of four ion chemistry steps were effected, three of which were ion/ion reaction steps and one of which was a collision-induced dissociation step. The spectrum reflects the dissociation products of a gas-phase concentrated and purified protein ion. This overall capability is attractive from the point of view of complex protein mixture analysis and is only possible due to the flexible nature of the system to devise the involved MS^n experiment required to provide it.

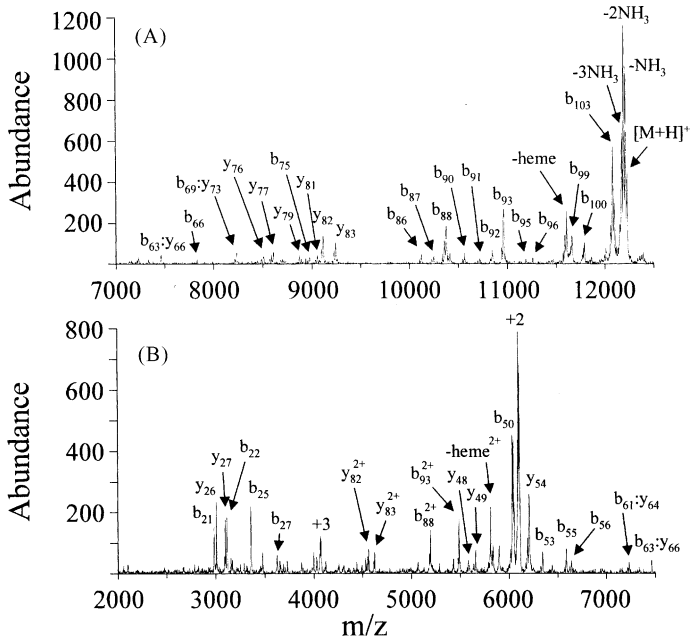

Fig. 8. Post-ion/ion reaction CID MS/MS spectrum of the $[M + 7H]^{7+}$ ion of cytochrome *c*, following concentration and purification from the $[M + 8H]^{8+}$ ion (Figs. 6 and 7), dissociation, and ion/ion reactions to reduce the product ions primarily to their singly-charged states. The spectrum was acquired under the same conditions as described in Fig. 3B.

4. Conclusions

The range of experiments and the quality of the results associated with ion/ion reactions involving multiply-charged ions are dependent upon mass analysis figures of merit and the flexibility in defining MS^n experiments. The instrument described herein provides an upper mass-to-charge ratio limit of roughly 150,000 and mass measurement accuracy of roughly 200 ppm or better below *m/z* 20,000. The mass resolving power is related inversely to the extent to which the upper mass-to-charge ratio limit is extended from the standard limit of *m/z* 2000. For an upper mass-to-charge ratio limit of 20,000, the mass resolving power is slightly better than 1500. These mass analysis figures of merit are better by factors of about 2–5 than those observed with older ion trap instrumentation.

The system allows for a wide range of possible MS^n experiments that can combine both collision-induced dissociation steps and ion/ion reactions. Sophisticated experiments involving sequential ion parking steps interspersed with ion isolation steps prior to a collisional activation step are straightforward to perform. Such a process can serve both to concentrate and to purify multiply-charged ions in the gas-phase at relatively high efficiencies (>80% illustrated here). The combination of improved mass analysis figures of merit with high flexibility in designing MS^n procedures gives rise to a powerful tool for studying and applying ion/ion reactions in the gas-phase.

Acknowledgements

This work was supported by the Integrated Detection of Hazardous Materials Program at Purdue University. We would like to thank Mr. Randy Replogle and Mr. Greg Hawkins for construction of the ASGDI source components, and Mr. Chris Doerge, of the

Amy Facility for Chemical Instrumentation, for construction of the custom amplifier circuit. We would also like to acknowledge Dr. Peter Grosshans and Mr. Craig Walla of Hitachi Instruments Inc. for providing custom instrument control software to support the ion/ion reaction studies and for technical advice in implementing novel aspects associated with these experiments.

References

[1] S.-W. Lee, P. Freivogel, T. Schindler, J.L. Beauchamp, J. Am. Chem. Soc. 120 (1998) 11758.
[2] S.-W. Lee, H.S. Kim, J.L. Beauchamp, J. Am. Chem. Soc. 120 (1998) 3188.
[3] M.T. Rodgers, S.A. Campbell, J.L. Beauchamp, Int. J. Mass Spectrom. Ion Process. 161 (1997) 193.
[4] M.T. Rodgers, S. Campbell, E.M. Marzluff, J.L. Beauchamp, Int. J. Mass Spectrom. Ion Process. 148 (1995) 1.
[5] M.T. Rodgers, S. Campbell, E.M. Marzluff, J.L. Beauchamp, Int. J. Mass Spectrom. Ion Process. 137 (1994) 121.
[6] E.M. Marzluff, S. Campbell, M.T. Rodgers, J.L. Beauchamp, J. Am. Chem. Soc. 116 (1994) 7787.
[7] E.M. Marzluff, S. Campbell, M.T. Rodgers, J.L. Beauchamp, J. Am. Chem. Soc. 116 (1994) 6947.
[8] S.-W. Lee, H.S. Kim, J.L. Beauchamp, J. Am. Chem. Soc. 120 (1998) 5800.
[9] S. Campbell, M.T. Rodgers, E.M. Marzluff, J.L. Beauchamp, J. Am. Chem. Soc. 117 (1995) 12840.
[10] S. Campbell, M.T. Rodgers, E.M. Marzluff, J.L. Beauchamp, J. Am. Chem. Soc. 116 (1994) 9765.
[11] M.B. Comisarow, A.G. Marshall, Chem. Phys. Lett. 25 (1974) 282.
[12] C.L. Hendrickson, M.R. Emmett, Ann. Rev. Phys. Chem. 50 (1999) 517.
[13] A.G. Marshall, C.L. Hendrickson, G.S. Jackson, Mass Spectrom. Rev. 17 (1998) 1.
[14] M.B. Comisarow, A.G. Marshall, J. Mass Spectrom. 31 (1996) 581.
[15] G.C. Stafford Jr., P.E. Kelley, J.E.P. Syka, W.E. Reynolds, J.F.J. Todd, Int. J. Mass Spectrom. Ion Process. 60 (1984) 85.
[16] R.E. March, R.J. Hughes, Quadrupole Storage Mass Spectrometry, Wiley, New York, 1989.
[17] R.E. March, J.F.J. Todd (Eds.), Practical Aspects of Ion Trap Mass Spectrometry, vols. I–III, CRC Press, Boca Raton, FL, 1995.
[18] R.E. Mather, J.F.J. Todd, Int J. Mass Spectrom. Ion Phys. 33 (1980) 159.
[19] J.D. Williams, R.G. Cooks, Rapid Commun. Mass Spectrom. 7 (1993) 380.
[20] J.B. Fenn, M. Mann, C.K. Meng, S.F. Wong, C.M. Whitehouse, Mass Spectrom. Rev. 9 (1990) 37.
[21] R.B. Cole (Ed.), Electrospray Ionization Mass Spectrometry, Wiley, New York, 1997.
[22] S.A. McLuckey, J.M. Wells, J.L. Stephenson Jr., D.E. Goeringer, Int. J. Mass Spectrom. 200 (2000) 137.
[23] S.A. McLuckey, J.L. Stephenson Jr., Mass Spectrom. Rev. 17 (1998) 369.
[24] J.L. Stephenson Jr., S.A. McLuckey, J. Am. Chem. Soc. 118 (1996) 7390.
[25] W.J. Herron, D.E. Goeringer, S.A. McLuckey, J. Am. Chem. Soc. 117 (1995) 11555.
[26] W.J. Herron, D.E. Goeringer, S.A. McLuckey, J. Am. Soc. Mass Spectrom. 6 (1995) 529.
[27] J.L. Stephenson Jr., S.A. McLuckey, Anal. Chem. 68 (1996) 4026.
[28] S.A. McLuckey, J.L. Stephenson Jr., K.G. Asano, Anal. Chem. 70 (1998) 1198.
[29] J.L. Stephenson Jr., S.A. McLuckey, Anal. Chem. 70 (1998) 3533.
[30] J.M. Wells, P.A. Chrisman, S.A. McLuckey, J. Am. Chem. Soc. 123 (2001) 12428.
[31] A.H. Payne, G.L. Glish, Int. J. Mass Spectrom. 204 (2001) 47.
[32] R.R.O. Loo, H.R. Udseth, R.D. Smith, J. Phys. Chem. 95 (1991) 6412.
[33] R.R.O. Loo, H.R. Udseth, R.D. Smith, J. Am. Soc. Mass Spectrom. 3 (1992) 695.
[34] M. Scalf, M.S. Westphall, J. Krause, S.L. Kaufman, L.M. Smith, Science 283 (1999) 194.
[35] M. Scalf, M.S. Westphall, L.M. Smith, Anal. Chem. 72 (2000) 52.
[36] D.D. Ebeling, M.S. Westphall, M. Scalf, L.M. Smith, Anal. Chem. 72 (2000) 5158.
[37] J.N. Louris, J.S. Brodbelt-Lustig, R.G. Cooks, G.L. Glish, G.J. Van Berkel, S.A. McLuckey, Int. J. Mass Spectrom. Ion Process. 96 (1990) 117.
[38] S.A. McLuckey, G.L. Glish, G.J. Van Berkel, Int. J. Mass Spectrom. Ion Process. 106 (1991) 213.
[39] T.G. Schaaff, B.J. Cargile, J.L. Stephenson Jr., S.A. McLuckey, Anal. Chem. 72 (2000) 899.
[40] J.M. Wells, J.L. Stephenson Jr., S.A. McLuckey, Int. J. Mass Spectrom. 203 (2000) A1.
[41] B.J. Cargile, S.A. McLuckey, J.L. Stephenson Jr., Anal. Chem. 74 (2001) 1277.
[42] G.E. Reid, J. Wu, P.A. Chrisman, J.M. Wells, S.A. McLuckey, Anal. Chem. 73 (2001) 3274.
[43] P.A. Chrisman, K.A. Newton, J.M. Wells, G.E. Reid, S.A. McLuckey, Int. J. Mass Spectrom. 212 (2001) 359.
[44] J.M. Wells, G.E. Reid, B.J. Engel, P. Pan, S.A. McLuckey, J. Am. Soc. Mass Spectrom. 12 (2001) 873.
[45] B.J. Engel, P. Pan, G.E. Reid, J.M. Wells, S.A. McLuckey, Int. J. Mass Spectrom. 219 (2002) 171.
[46] G.E. Reid, J.L. Stephenson Jr., S.A. McLuckey, Anal. Chem. 74 (2002) 577.
[47] S.A. McLuckey, G.E. Reid, J.M. Wells, Anal. Chem. 74 (2002) 336.
[48] G.E. Reid, H. Shang, J. Hogan, G.U. Lee, S.A. McLuckey, J. Am. Chem. Soc. 124 (2002) 7353.

[49] M. He, G.E. Reid, H. Shang, G.U. Lee, S.A. McLuckey, Anal. Chem. 74 (2002) 4653.
[50] J.L. Stephenson Jr., S.A. McLuckey, G.E. Reid, J.M. Wells, J.L. Bundy, Curr. Opin. Biotech. 13 (2002) 57.
[51] G.E. Reid, S.A. McLuckey, J. Mass Spectrom. 37 (2002) 663.
[52] S.A. McLuckey, G.L. Glish, K.G. Asano, B.C. Grant, Anal. Chem. 60 (1988) 2220.
[53] S.A. McLuckey, J.M. Wells, Chem. Rev. 101 (2001) 571.
[54] P.E. Kelley, U.S. Patent 5,134,286 (1992).
[55] D.E. Goeringer, K.G. Asano, S.A. McLuckey, D. Hoekman, S.E. Stiller, Anal. Chem. 66 (1994) 313.
[56] R.E. Kaiser Jr., R.G. Cooks, J. Moss, P.H. Hemberger, Rapid Commun. Mass Spectrom. 3 (1989) 50.
[57] R.E. Kaiser Jr., R.G. Cooks, G.C. Stafford Jr., J.E.P. Syka, P.H. Hemberger, Int. J. Mass Spectrom. Ion Process. 106 (1991) 79.
[58] N. Yates, ICMS software, University of Florida.
[59] J.L. Stephenson Jr., S.A. McLuckey, Int. J. Mass Spectrom. Ion Process. 162 (1997) 89.
[60] Y. Wang, M. Schubert, A. Ingendoh, J. Franzen, Rapid Commun. Mass Spectrom. 14 (2000) 12.
[61] U.P. Schlunegger, M. Stoeckli, R.M. Caprioli, Rapid Commun. Mass Spectrom. 13 (1999) 1792.
[62] Y. Cai, W.-P. Peng, S.-J. Kuo, Y.T. Lee, H.-C. Chang, Anal. Chem. 74 (2002) 232.
[63] F.G. Major, H.G. Dehmelt, Phys. Rev. 179 (1968) 91.